AGU PUBLICATIONS

Geophysical Research Letters

RESEARCH LETTER
10.1002/2016GL070876

Key Points:
- We develop a new system for continuous noble analysis during rock deformation
- We measure radiogenic noble release from rocks undergoing triaxial deformation
- Radiogenic noble gas release is tightly coupled to the state of stress and strain in rocks

Correspondence to:
W. P. Gardner,
payton.gardner@mso.umt.edu

Citation:
Bauer, S. J., W. P. Gardner, and H. Lee (2016), Release of radiogenic noble gases as a new signal of rock deformation, *Geophys. Res. Lett.*, *43*, 10,688–10,694, doi:10.1002/2016GL070876.

Received 16 AUG 2016
Accepted 6 OCT 2016
Accepted article online 9 OCT 2016
Published online 27 OCT 2016

Release of radiogenic noble gases as a new signal of rock deformation

Stephen J. Bauer[1], W. Payton Gardner[2], and Hyunwoo Lee[3]

[1]Geomechanics Department, Sandia National Laboratories, Albuquerque, New Mexico, USA, [2]Department of Geosciences, University of Montana, Missoula, Montana, USA, [3]Department of Earth and Planetary Sciences, University of New Mexico, Albuquerque, New Mexico, USA

Abstract In this study we investigate the release of radiogenic noble gas isotopes during mechanical deformation. We developed an analytical system for dynamic mass spectrometry of noble gas composition and helium release rate of gas produced during mechanical deformation of rocks. Our results indicate that rocks release accumulated radiogenic helium and argon from mineral grains as they undergo deformation. We found that the release of accumulated ^{4}He and ^{40}Ar from rocks follows a reproducible pattern and can provide insight into the deformation process. Increased gas release can be observed before dilation, and macroscopic failure is observed during high-pressure triaxial rock deformation experiments. Accumulated radiogenic noble gases can be released due to fracturing of mineral grains during small-scale strain in Earth materials. Helium and argon are highly mobile, conservative species and could be used to provide information on changes in the state of stress and strain in Earth materials, and as an early warning signal of macroscopic failure. These results pave the way for the use of noble gases to trace and monitor rock deformation for earthquake prediction and a variety of other subsurface engineering projects.

1. Introduction

A signal of microscopic failure during strain and dilation has long been sought as a precursor to large-scale rock failure such as earthquakes. As rocks deform, microfracturing at the grain scale begins when a rock reaches half of its yield strength. These microfractures become more pervasive as the rock undergoes dilation and finally coalesce into a through-going fracture during macroscopic failure. Microfracture and dilation could release naturally produced, stable radiogenic helium and argon isotopes, providing a signal of strain which precedes macroscopic failure. However, to date the release of helium and argon from rocks undergoing deformation has not been reported.

Geochemical signals of prerupture deformation have been thought to provide a potential means to forecast earthquakes since variations in radon were observed before earthquakes in Japan [*Wakita et al.*, 1980] and Hawaii [*Cox et al.*, 1980]. Radon concentrations in groundwater and soil gases have been shown to decrease [*Wakita et al.*, 1980, 1991] and/or increase [*Cox et al.*, 1980], while groundwater chemical and stable isotopic composition has been noted to change prior to seismicity [*Tsunogai and Wakita*, 1995; *Skelton et al.*, 2014]. These geochemical signals are hypothesized to arise due to mechanical deformation of the subsurface including slow strain, dilation, and microfracturing, which can increase radon emanation from rocks, coupled with stress-related changes in the permeability field which cause changes in groundwater flow paths and mixing. Radon emanation from rocks undergoing uniaxial deformation has been observed to increase in the laboratory as new fractures are formed [*Holub and Brady*, 1981; *Tuccimei et al.*, 2010] but does not increase during subsequent deformation after fracture formation [*Mollo et al.*, 2011], indicating that radiogenic gas release can provide information on the current state and history of strain. At the field scale, radon bursts have been detected in tunnel air as a result of nonseismogenic stress and strain during seasonal hydrological loading of the shallow subsurface [*Trique et al.*, 1999].

Previous results indicate that geochemical signals could be used to understand changes in subsurface stress and strain; however, the travel distance of the radon signal is limited by radioactive decay, while major ion and stable isotope signals are limited by water-rock reaction kinetics, thus, probably only indicate changes in subsurface flow path distribution. Noble gases have isotopically distinct compositions in mantle, crustal, and atmospheric reservoirs and are commonly used to trace geochemical and crustal fluid migration

[*Porcelli et al.*, 2002]. ^{4}He, ^{40}Ar, and other radiogenic noble gases accumulate in mineral grains due to the decay of naturally occurring radioactive elements in crustal materials [*Lehmann et al.*, 2003; *Tolstikhin et al.*, 1996] and are transferred to the adjacent pore fluid by diffusion, recoil, and mineral dissolution [*Torgersen*, 1980]. The role of stress and deformation on the release of radiogenic helium and argon from minerals is largely unknown, but field evidence exists to suggest that it is coupled to mechanical processes. Helium concentration and isotopic composition in subsurface fluids have been traced to tectonic deformation processes at the continental scale [*Kennedy and van Soest*, 2007]. Postseismic helium isotope variations in groundwater have been detected [*Brauer et al.*, 2003] and attributed to mechanical processes due to seismicity. Accumulated crustal helium is released due to volcanic activity over geologic time scales [*Lowenstern et al.*, 2014], and helium diffusive degassing has been shown to increase prior to volcanic eruptions [*Padrón et al.*, 2013]. The release of radiogenic noble gases, particularly helium, from mineral grains and immobile pore volumes, as a result of fracturing during deformation could be an ideal signal of subsurface deformation as helium is highly mobile, stable, and of low concentration in atmospheric waters. However, the effect of stress and strain on helium release from rocks has never been quantified.

Here we present the first results of the real-time release of naturally occurring ^{4}He and ^{40}Ar from rocks as they undergo deformation. We use a unique experimental capability to continuously monitor the gas composition of rocks as they undergo triaxial deformation. From our experiments it is clear that stress and strain play an important role in the release of radiogenic noble gases from mineral grains and that the release of these gases is a sensitive tracer of the state of stress and strain in rocks. We propose that radiogenic noble gas release could be used as a new signal of stress and strain with implications across a diverse set of Earth sciences including earthquake hazard prediction, strain monitoring in subsurface engineering, and studies of hydromechanical coupling.

2. Methods

We developed an analytical system capable of measuring either helium release or noble gas composition of released gases from rocks as they undergo high-pressure triaxial deformation. This system was used to make high-resolution, continuous measurements of the helium release rate, or the noble gas composition of gases released from rocks undergoing triaxial deformation. Helium release rate was measured with a mass spectrometer leak detector connected to the pore volume of the rock specimens. Noble gas isotopic composition of released gases was measured by connecting a high-resolution quadrupole mass spectrometer with continuous, dynamic gas inlet and cross-beam ion source, to the specimen pore space. Gas composition or release rate was measured along with traditional measurements of triaxial stress and strain and acoustic emissions.

We measured gas release from right circular cylinder core specimens taken from previously quarried Westerly granite, a fine-grained granodiorite. This rock type was chosen because the mechanical properties have been studied extensively [*Krech et al.*, 1974], and it is known to contain fluid inclusions in the mineral grains [*Hall and Bodnar*, 1989]. For these samples, shelf storage times have allowed accumulated radiogenic noble gases in the pore volume to equilibrate with the atmosphere via diffusion, but mineral grains will have retained radiogenic gases. Our hypothesis was that crystalline rock deformation will release residual atmospheric gases in the pore space radiogenic gases accumulated within mineral grains and fluid inclusions due to lattice deformation via fracturing.

2.1. Analytical Methods

The mechanical portion of the test system consists of a triaxial pressure cell which can be placed in a variety of loading frames, with the capability of triaxial testing of cylindrical samples ranging in diameter from 2.5 cm diameter (5 cm long) to 10 cm diameter (20–25 cm in length). The triaxial cells are capable of confining pressures to 400 MPa with sufficient axial force (stress) capabilities to fracture rock in compression/extension. The mechanical test system has a pore fluid flow-through capability used with high pressure (to simulate pore pressure at depth) which we modified in the present application to apply vacuum to the rock pore space. The reaction frame used is capable of applying loads up to 4.45 MN through a hydraulic actuator in the base of the frame. Confining pressure was measured with a pressure transducer plumbed directly into the hardline that connects the pressure vessel to the pressure intensifier. The transducer is located about 1.5 m from the vessel pressure. Data collected in the experimental study included force, pressure, temperature, axial and

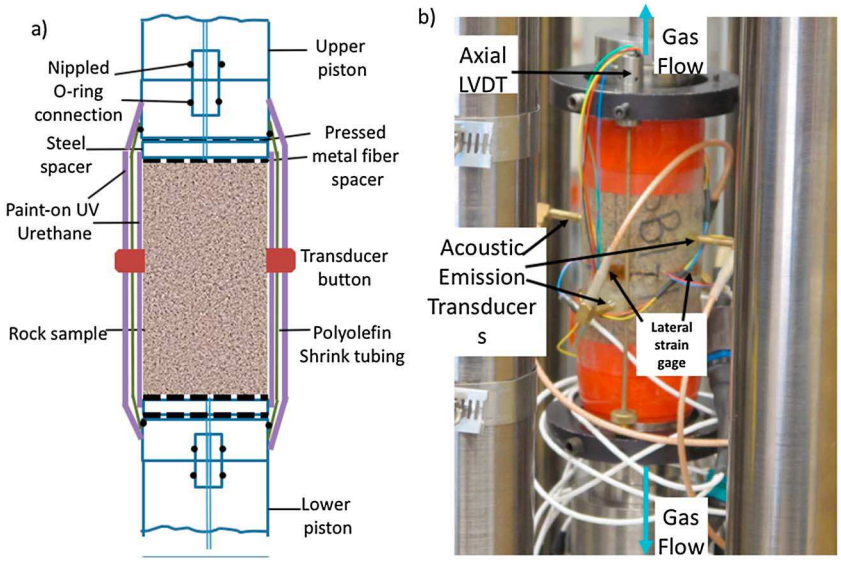

Figure 1. Typical sample assembly: (a) Schematic; (b) actual.

lateral displacements, gas release, acoustic emissions, and vacuum pressure. Data are acquired using electronic transducers in which voltage is proportional to the change in the measured variable. In all cases, the constants of proportionality were determined through careful calibration using National Institute of Standards and Technology traceable standards.

The residual gas analysis portion of the test system utilizes two different mass spectrometers: a quadrupole mass spectrometer capable of scanning the total abundance of gas over a broad mass range and a helium leak detector specifically tuned to mass 4 amu, which measures the flow rate of helium. The quadrupole mass spectrometer is a Pfeiffer HiQuad^{TM} for analysis of neutral particles with a mass range from 1 to 340 amu. The scan speed is 0.125 ms to 60 s/amu, typically full scan time for a suite of gases (10 species) is on the order of 1–2 s. The mass filter utilizes 16 mm molybdenum rods for maximum selectivity, with a cross-beam ion source with tungsten filament for maximum sensitivity during dynamic measurements. A focusing dynode electron multiplier was used as the detector for maximum linearity over pressure ranges from 10^{-15} to 10^{-6} mbar. The minimum partial pressure detection limit for this instrumental configuration is 1×10^{-15} mbar. The helium leak detector is an Oerlikon Leibold Phoenix L300i, a specialized mass spectrometer tuned to 4 amu to observe helium release rates, with a minimum detectable leak rate in vacuum mode at $<5\times10^{-12}$ mbar l/s. The temporal resolution of the leak rate signal is <1 s, and the filament is Iridium/Yttria oxide.

In order to protect the vacuum system in the event of a confining fluid leak, low positive pressure (0.1–0.2 MPa), high-vacuum relief valves, and a high-vacuum fluid expansion trap designed to accommodate the decompression of the confining fluid from the maximum confining pressure to 0.1 MPA were included in the vacuum system. Helium leak rate standards were used to blackcalibrate the leak detector, and atmosphere was used as a standard to calibrate the mixing fractions for the quadrupole mass spectrometer.

2.2. Experimental Design

Rock core samples were assembled as shown in Figure 1. The rock sample is ground for parallel and perpendicular conditions per ASTM standards. The samples were right circular cylinders of Westerly granite, nominally 3.8 cm in diameter, 8 cm in length and weighing between 250 and 260 g and were oven dried for a week at 50°C prior to testing. Acoustic emission transducer buttons were glued directly to the sample along a diameter near the sample midheight. The sample was sandwiched between alternating layers of pressed metal fiber mesh and steel spacers to assure gas flow accessibility along the core ends. The sample is then jacketed to keep confining fluid out of the pore volume. Specimens were jacketed first with a thin layer of UV cure urethane which adheres tightly to the rock surface inhibiting gas flow along the rock surface. A sleeve of polyolefin shrink tube was placed over the first layer of UV cure urethane, and then encapsulated in another layer of UV cure urethane. This jacketing procedure has proved successful in avoiding jacket leaks during rock fracture events.

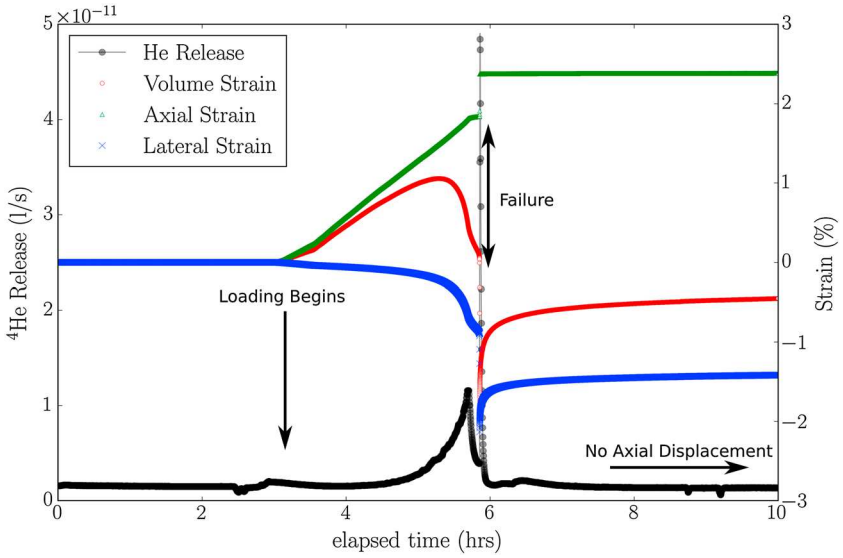

Figure 2. Helium release rate as measured by the helium leak detector and volume strain for Westerly granite experiment 3 (WG3).

Test specimens are instrumented to measure axial and radial displacements. Displacement is measured with four Linear Variable Differential Transformers (LVDTs): two LVDTs mounted on the end caps to measure axial deformation, and two mounted in spring loaded rings placed near the sample midheight to measure change in diameter (Figure 1). LVDT displacements are averaged to calculate strain; the actuator has a separate LVDT that can be used as a backup to on-sample axial measurements. Sample mounted LVDTs have a total displacement scale of 0.254 cm. Displacement is used to calculate sample strain and stress calculated using the measured force and updated cross-sectional area based on lateral displacements.

Jacketed and instrumented specimens were plumbed into the base of the pressure vessel and connected to pore pressure feed throughs out the top of the pressure vessel. The pressure vessel was then assembled and placed into the reaction frame. The actuator in the base of the frame was raised gradually to bring the pressure vessel piston into contact with the reaction frame. The pressure vessel was then connected to the pressure intensifier and filled with Isopar®. At this point the servohydraulic control was turned on and data collection begun. The confining pressure was raised to 13.8 MPa, with the reaction frame actuator holding its position. The vacuum line was then connected to the pore pressure system, allowing gas sampling access from both the top and bottom of the specimen during deformation. After pressurization and vacuum pump down—helium leak rate or gas composition was monitored for at least 24 h to measure the background conditions.

During the experiment, confining pressure was controlled, measured, and tracked using the pressure transducer located in the intensifier connection line about 1.5 m from the pressure vessel. Axial force is measured with a load cell external to the pressure vessel and O-ring friction was corrected for during data analysis. The specimen was deformed using a controlled displacement mode and shortened at a rate of approximately 5×10^{-6} s^{-1}. Force, displacement, confining pressure, acoustic emissions, helium leak rate, or gas compositions were recorded in an automatic data acquisition/control system as a function of time.

In this paper we report on the results of three separate deformation experiments, each testing a different aspect of deformation and gas release. In experiment WG3, we performed a full deformation through macroscopic fracture measuring the total ^{4}He release rate with the leak detector. In experiment WG1, we performed a full deformation through macroscopic fracture measuring the composition of evolved gases during deformation with the quadrupole. Finally, in WG7, we deformed a specimen from elastic through plastic deformation stopping just prior to macrofailure and recorded acoustic emissions along with the helium release rate with the leak detectors.

Specimens were prepared, placed in the pressure vessel, brought to the desired hydrostatic confining pressure and background gas composition or leak rate measured for over 24 h. Triaxial deformation was then initiated and the gas composition or leak rate measured continuously throughout specimen deformation until

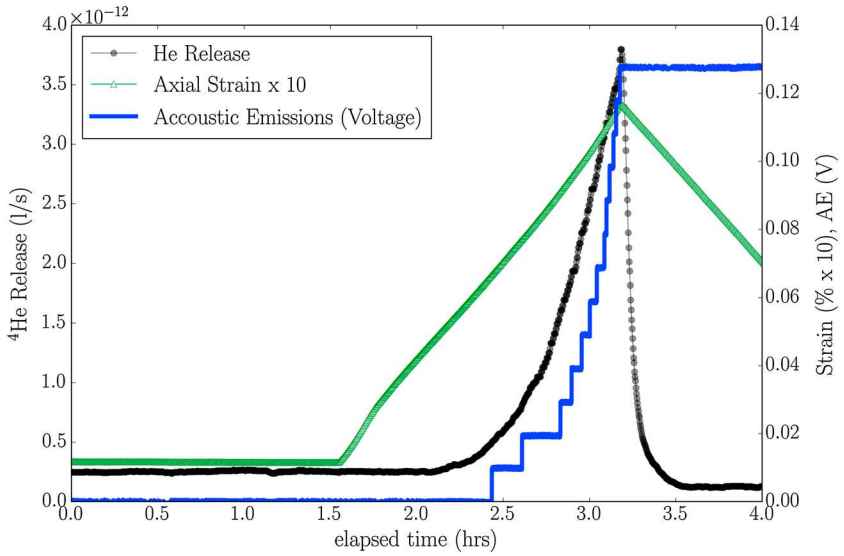

Figure 3. Helium release rate and accumulated acoustic emissions for Westerly granite experiment 4 (WG7) for strain prior to macroscopic failure.

macroscopic failure, after which deformation was halted and the gas composition or leak rate monitored for a minimum of an additional 24 h.

3. Results

Helium release during deformation was observed to follow a systematic pattern indicative of the mechanical processes effective during different stages of deformation (Figure 2). During the initial portions of the deformation, axial loading and elastic compaction are the dominant deformation modes, causing mechanically induced reduction of the pore volume and intrinsic permeability of the rock. During this portion of the experiment a subsequent continuous reduction in the ^{4}He release rate from the rock was observed. At roughly one third to one half of the total prefailure yield strength (an elapsed time of ~4.5 h, Figure 2), the ^{4}He release rate reaches a minimum. After this point the helium release rate then begins to increase indicating formation of intragranular microfractures. This rise is coincident with the initiation of microcracking as recorded by acoustic emissions (elapsed time ~2.5 h, Figure 3). The acoustic emission signal shows large steps indicative of large, discrete fracturing events. Small fracturing events below detection limits could be occurring between the larger acoustic emission events (Figure 3). During this phase, the ^{4}He release rate is observed to increase up to 100% before any signs of macroscopic failure become evident. The helium flow steadily increases until the failure point due to coalescence of microfractures from rupture of mineral grains and fluid inclusions and the subsequent increase in diffusive surface area and specimen permeability as a result of fracturing (Figure 4). After specimen macrofracture, axial displacement was halted and held, and the helium release rate decreased back down to values near or slightly above the predeformation value.

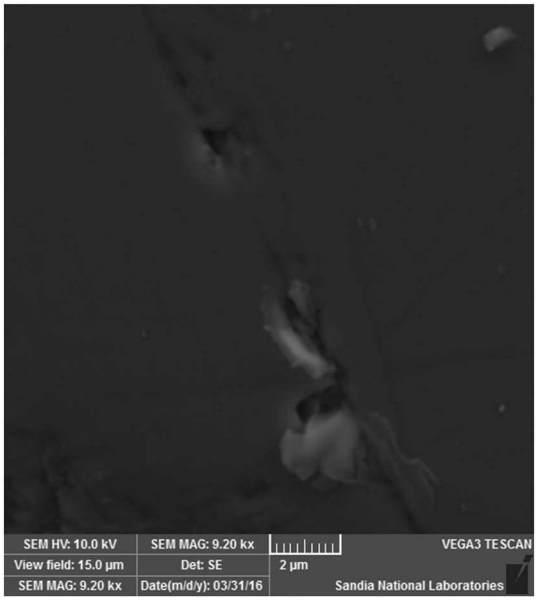

Figure 4. Post test scanning electron microscope image of microfracture intersecting a pore from the WG1 core.

The composition of gases released from the Westerly granite show a dynamic response

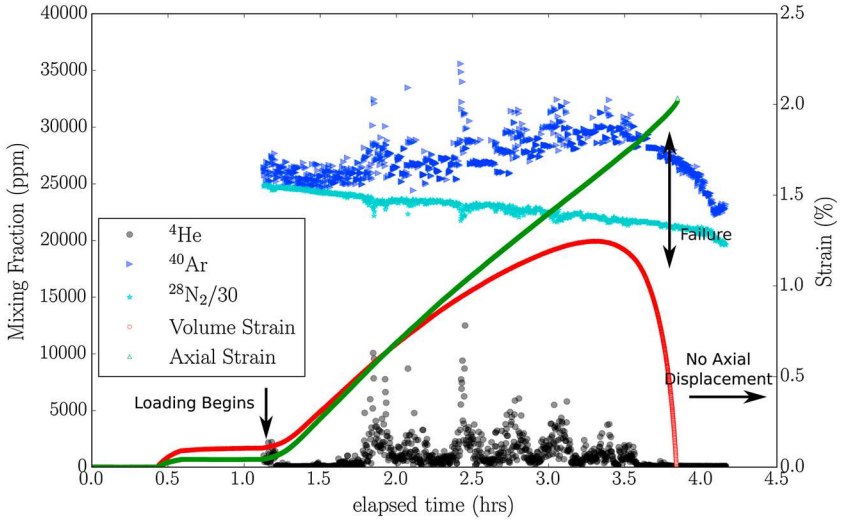

Figure 5. Mixing fraction of ^{4}He and ^{40}Ar in released gas along with strain for Westerly granite experiment (WG1).

indicative of release of radiogenic gases in discrete microfracturing events (Figure 5). After some small variability during initial loading of the sample, the gas composition remains relatively constant for the first third of the accumulating elastic volume strain (roughly 1.75 h elapsed time, Figure 5), at which point discrete bursts of gas with higher ^{4}He and ^{40}Ar partial pressures become apparent. During these discrete gas burst events, the ^{4}He to $^{28}N_2$ ratio increases, consistent with grain rupture releasing gas from a radiogenic reservoir. The gas bursts occur steadily from their initiation point until deformation is halted, after which the ^{4}He and ^{40}Ar partial pressures return toward their original values. The release pattern observed is consistent with fracturing of individual mineral grains which releases radiogenic gases. The difference in response time between the leak detector and the quadrupole can be explained by the leak detector's dynamic ranging features, which open and close valves depending upon the inlet pressure decreasing instrumental response time. In contrast, the quadrupole system remains in a constant fully open configuration.

4. Discussion and Conclusion

Our analytical capabilities have allowed us to make observations on the effects of mechanical stress and deformation on the release of accumulated radiogenic noble gases from rocks. The release of radiogenic noble gases from deforming crystalline rocks has a distinct, reproducible pattern and provides a sensitive signal of the deformation processes at work. We recorded a well over 100% increase in the helium release rate from rock samples in advance of any macroscopic signal of failure (a stress drop). In fact, the reproducibility and sensitivity of this signal is strong enough that we have begun to use the gas release signal as an indicator of strain and microcracking in our deformation experiments rather than more traditional stress and strain data. The release pattern we observed is consistent with our previous work with artificially doped shale gas reservoir rocks [*Bauer et al.*, 2016] and past experiments recording radon exhalation rates from rocks undergoing deformation [*Holub and Brady*, 1981; *Tuccimei et al.*, 2010; *Mollo et al.*, 2011]; however, by using helium and argon as opposed to ^{222}Rn, we achieve significantly better temporal resolution as we are not limited by decay counting rates for detection. These gases appear to be released in discrete cracking events, which is consistent with field scale observations of ^{222}Rn bursts in tunnel air [*Trique et al.*, 1999].

Radiogenic production of noble gases and their release have been utilized in a variety of ways for understanding the movement of groundwater and other crustal fluids. In order to use these tracers, the production rate and the transfer processes from the mineral grain to adjacent pore fluid must be known. To date the transfer processes which have been considered are alpha recoil, diffusion, and chemical dissolution. These experiments show that small-scale strain and fracturing, even well below the ultimate yield strength of the rock, can release accumulated noble gases; thus, the state of stress and strain is tightly coupled to the concentration of radiogenic noble gases in pore fluids. This coupling is a new process which should be considered when interpreting noble gases as fluid tracers.

We calculate an estimate of the signal strength for helium released during fracture assuming that 30% of mineral grains rupture. Assuming that we can detect a 10% increase in helium over background concentrations, and that the rock concentration is similar to the Carmenellis granite [*Hussain*, 1997], we estimate that the volume of fracture must be greater than 1% of the total mixing volume from which a sample is taken, for a distinctly observable signal. Increased diffusive release from the matrix to the fracture network and enhanced matrix permeability also enhance the signal strength. A 1 order of magnitude increase in permeability due to microfracturing would increase radiogenic gas release by roughly 1 order of magnitude, bringing the total cracking volume required for an observable signal to 0.1% or less of the total mixing volume.

Our results have multiple implications across the Earth and engineering sciences. The degassing rate of noble gases from crystalline rocks is clearly dependent upon the evolving state of stress and strain. The noble gas release patterns observed were systematic and reveal information on the deformation processes at work and can be observed well before traditional measures of macroscopic failure. In addition to developing a new process to be considered when interpreting noble gases in crustal fluids, we lay the foundation for a new signal to monitor changes in stress and strain at a variety of scales in both subsurface and engineered materials. Changes in the release of ^{4}He or other radiogenic noble gases could provide an early warning system for detecting changes in microcrack-related permanent strain and subsequent dilation precursive to macroscopic failure such as earthquakes or mine failure. As humans undertake larger and more complex subsurface engineering projects as a result of energy and natural resource production and/or waste disposal, new signals for monitoring changes in the stress and strain field are required; these results set the stage for utilizing radiogenic noble gases as a signal to sense changes in mechanical deformation of the subsurface.

Acknowledgments
Sandia National Laboratories is a multiprogram laboratory managed and operated by Sandia Corporation, a wholly owned subsidiary of Lockheed Martin Corporation, for the U.S. Department of Energy's National Nuclear Security Administration under contract DE-AC04-94AL85000. We would like to thank the Sandia LDRD program for funding our initial study and equipment purchase. The data used are available upon request from the authors. Correspondence and requests for data and materials should be addressed to W. Payton Gardner (email: payton.gardner@umontana.edu).

References

Bauer, S. J., W. P. Gardner, and J. E. Heath (2016), Helium release during shale deformation: Experimental validation, *Geochem. Geophys. Geosyst.*, *17*, 2612–2622, doi:10.1002/2016GC006352.

Brauer, K., H. Kampf, G. Strauch, and S. M. Weise (2003), Isotopic evidence (^{3}He/^{4}He, $^{13}C_{CO_2}$) of fluid-triggered intraplate seismicity, *J. Geophys. Res.*, *108*(B2), 2070, doi:10.1029/2002JB002077.

Cox, M. E., K. E. Cuff, and D. M. Thomas (1980), Variations of ground radon concentrations with activity of Kilauea Volcano, Hawaii, *Nature*, *288*(5786), 74–76.

Hall, D. L., and R. J. Bodnar (1989), Comparison of fluid inclusion decrepitation and acoustic emission profiles of Westerly granite and Sioux quartzite, *Tectonophysics*, *168*(4), 283–296, doi:10.1016/0040-1951(89)90223-0.

Holub, R. F., and B. T. Brady (1981), The effect of stress on radon emanation from rock, *J. Geophys. Res.*, *86*(B3), 1776–1784, doi:10.1029/JB086iB03p01776.

Hussain, N. (1997), Flux of ^{4}He from Carnmenellis granite: Modelling of an HDR geothermal reservoir, *Appl. Geochem.*, *12*(1), 1–8, doi:10.1016/S0883-2927(96)00038-8.

Kennedy, B. M., and M. C. van Soest (2007), Flow of mantle fluids through the ductile lower crust: Helium isotope trends, *Science*, *318*(5855), 1433–1436, doi:10.1126/science.1147537.

Krech, W. W., K. E. Hjelmstad, and F. A. Henderson (1974), *A Standard Rock Suite for Rapid Excavation Research, II*, 29 pp., U.S. Bureau of Mines, Washington, D. C.

Lehmann, B. E., H. N. Waber, I. Tolstikhin, I. Kamensky, M. Gannibal, E. Kalashnikov, and B. Pevzner (2003), Helium in solubility equilibrium with quartz and porefluids in rocks: A new approach in hydrology, *Geophys. Res. Lett.*, *30*(3), 1128, doi:10.1029/2002GL016074.

Lowenstern, J. B., W. C. Evans, D. Bergfeld, and A. G. Hunt (2014), Prodigious degassing of a billion years of accumulated radiogenic helium at Yellowstone, *Nature*, *506*(7488), 355–358.

Mollo, S., P. Tuccimei, M. J. Heap, S. Vinciguerra, M. Soligo, M. Castelluccio, P. Scarlato, and D. B. Dingwell (2011), Increase in radon emission due to rock failure: An experimental study, *Geophys. Res. Lett.*, *38*, L14304, doi:10.1029/2011GL047962.

Padrón, E., et al. (2013), Diffusive helium emissions as a precursory sign of volcanic unrest, *Geology*, *41*(5), 539–542, doi:10.1130/G34027.1.

Porcelli, D., C. J. Ballentine, and R. Wieler (Eds.) (2002), *Noble Gases in Geochemistry and Cosmochemistry, Reviews in Mineralogy and Geochemistry* , vol. 47, Mineral. Soc. of Am., Washington, D. C.

Skelton, A., et al. (2014), Changes in groundwater chemistry before two consecutive earthquakes in Iceland, *Nat. Geosci.*, *7*(10), 752–756.

Tolstikhin, I., B. E. Lehmann, H. H. Loosli, and A. Gautschi (1996), Helium and argon isotopes in rocks, minerals and related groundwaters: A case study in northern Switzerland, *Geochim. Cosmochim. Acta*, *60*(9), 1497–1514.

Torgersen, T. (1980), Controls on pore-fluid concentration of ^{4}He and ^{222}Rn and the calculation of ^{4}He/^{222}Rn ages, *J. Geochem. Expl.*, *13*(1), 57–75, doi:10.1016/0375-6742(80)90021-7.

Trique, M., P. Richon, F. Perrier, J. P. Avouac, and J. C. Sabroux (1999), Radon emanation and electric potential variations associated with transient deformation near reservoir lakes, *Nature*, *399*(6732), 137–141.

Tsunogai, U., and H. Wakita (1995), Precursory chemical changes in ground water: Kobe earthquake, Japan, *Science*, *269*(5220), 61–63.

Tuccimei, P., S. Mollo, S. Vinciguerra, M. Castelluccio, and M. Soligo (2010), Radon and thoron emission from lithophysae-rich tuff under increasing deformation: An experimental study, *Geophys. Res. Lett.*, *37*, L05305, doi:10.1029/2009GL042134.

Wakita, H., Y. Nakamura, K. Notsu, M. Noguchi, and T. Asada (1980), Radon anomaly: A possible precursor of the 1978 Izu-Oshima-Kinkai earthquake, *Science*, *207*(4433), 882–883.

Wakita, H., G. Igarashi, and K. Notsu (1991), An anomalous radon decrease in groundwater prior to an M6.0 earthquake: A possible precursor?, *Geophys. Res. Lett.*, *18*(4), 629–632, doi:10.1029/91GL00824.